Advances in Physics: X

ISSN: (Print) (Online) Journal homepage: https://www.tandfonline.com/loi/tapx20

# Electromagnetically induced transparency quantum memory for non-classical states of light

Xing Lei, Lixia Ma, Jieli Yan, Xiaoyu Zhou, Zhihui Yan & Xiaojun Jia

**To cite this article:** Xing Lei, Lixia Ma, Jieli Yan, Xiaoyu Zhou, Zhihui Yan & Xiaojun Jia (2022) Electromagnetically induced transparency quantum memory for non-classical states of light, Advances in Physics: X, 7:1, 2060133, DOI: 10.1080/23746149.2022.2060133

**To link to this article:** https://doi.org/10.1080/23746149.2022.2060133



Published online: 17 Apr 2022.

ADVANCES IN PHYSICS: X
2022, VOL. 7, NO. 1, 2060133
https://doi.org/10.1080/23746149.2022.2060133

Taylor & Francis
Taylor & Francis Group

REVIEW



# Electromagnetically induced transparency quantum memory for non-classical states of light

Xing Lei[a], Lixia Ma[a], Jieli Yan[a], Xiaoyu Zhou[a], Zhihui Yan[a,b] and Xiaojun Jia[a,b]

[a]State Key Laboratory of Quantum Optics Quantum Optics Devices, Institute of Opto-Electronics, Shanxi University, Taiyuan P. R. China; [b]Collaborative Innovation Center of Extreme Optics, Shanxi University, Taiyuan P. R. China

**ABSTRACT**

Quantum memory (QM) enables quantum state mapping between flying and stationary quantum states and is the building block of quantum information science, which enables to achieve a plethora of quantum information protocols, such as quantum state transfer across remote quantum nodes, distributed quantum logic gate, and quantum precession measurement network. Great progresses of quantum memories have been achieved, and electromagnetically induced transparency (EIT) is one of the well-understood approaches of QM. Quantum states of light are the essential quantum resources for implementing quantum enhanced task, and thus it is a long-standing goal to store and release non-classical states of light. This paper presents an up-to-date review on recent developments in EIT-based QM: EIT quantum memories have been realized in warm atomic cell, cold atoms and solid system, respectively; and EIT mechanism has been applied to store and release single photon, squeezed state, entangled photon pairs and multipartite entangled states of optical modes.

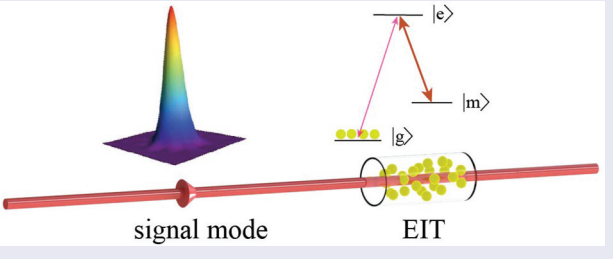


**ARTICLE HISTORY**
Compiled March 25, 2022

**KEYWORDS**
Quantum memory; electromagnetically induced transparency; non-classical states of light

## 1. Introduction

In quantum information science, quantum network can outperform the classical approaches for fast processing, secure communication and precision measurement by making use of their quantum advantages. Like

**CONTACT** Xiaojun Jia jiaxj@sxu.edu.cn State Key Laboratory of Quantum Optics Quantum Optics Devices, Institute of Opto-Electronics, Shanxi University, Taiyuan 030006, P. R. China; Collaborative Innovation Center of Extreme Optics, Shanxi University, Taiyuan 030006, P. R. China

classical network, quantum network consists of quantum channels and quantum nodes. Light is used to transfer quantum information in quantum channel across quantum network due to its fast transmission speed and weak interaction with the environment [1–3]. A variety of physical systems, such as atomic ensembles [4–8], single atom [9,10], trapped ions [11,12], superconductors [13], opto-mechanics [14–17] and crystals [18,19], can be used as quantum nodes to store and process quantum information. In the quantum internet, the loss and decoherence are unavoidable, which limits its performance and scale.

Quantum repeater consists of entanglement purification, entanglement swapping and quantum memory (QM), divides the entanglement distribution into short distance segments in order to overcome the above problems [20]. High-performance quantum computation requires large-scale quantum computers, which are also hindered by unavoidable decoherence. Besides fault-tolerant quantum computation, the distributed quantum computation paves another avenue to make quantum computation possible. By dividing a larger computing cluster into smaller quantum modules, distributed quantum module structure can solve the unavoidable decoherence problem, where the QM-based element registers can preserve, control and read out quantum states [21]. In precision measurement, the ultimate measurement sensitivity is limited by the quantum noise limit (QNL). Spin squeezing that can be produced by storing the squeezed state provides an effective approach to make sensitivity of atomic magnetometry to surpass this limit [22]. Therefore, QM is the essential quantum resource for the practical applications of quantum information science.

A variety of progress on quantum memories have been achieved including different kinds of light and atom interaction mechanisms, such as electromagnetically induced transparency (EIT) [23–25], quantum nondemolition (QND) [26], gradient echo memory [27,28], atomic frequency comb (AFC) [29], Raman scattering [20,30] and controlled reversible inhomogeneous boarding (CRIB) [31]. QM enables to map quantum state from the flying optical mode to stationary matter system and on demand releases it and vice versa. An EIT phenomenon induced by strong optical mode in an opaque medium due to quantum interference is suitable for storing and releasing quantum state of light on demand [23]. When quantum fields propagate in EIT media, there form dark-state polaritons, and the quantum states can be transferred between light and collective atomic excitations [32,33]. The long-lived spin states with high atomic densities in warm cesium (Cs) cell have been used to store the light onto spin orientation within a decoherence-free subspace of spin states, and its storage time can reach one second [34]. In QM, the memory efficiency is another key factor for the successful implementing of quantum state mapping. Warm atomic cell is one of the ideal candidates of memory media due to the simple

structure and easy operation. The efficiency above 40% for the storage and releasing with the optimal input signal mode shapes in warm rubidium (Rb) atomic cell have been realized based on the time-reversal procedure [35]. The laser cooled atoms provide another memory platform with the good coherence. By optimizing the optical depth (OD), a memory efficiency of 92% for coherent optical memory in optically dense cold atomic media has been realized [36]. A QM for polarization qubits encoded with weak coherent states at the single-photon level with an average conditional fidelity above 99% and efficiency around 68% has been implemented with spatially multiplex in an elongated laser-cooled ensemble of Cs atoms [37]. Besides, the solid system is suitable for practical application of QM. The storage and retrieval of light pulses in a $Pr^{3+}$:$Y_2SiO_5$ crystal have been demonstrated, and the memory efficiency reaches 76.3% when the OD is increased to 84 by using a ring-type configuration [38].

Quantum information includes the discrete variable (DV) and continuous variable (CV) approaches, whose observables are with the discrete and continuous eigenvalues, respectively. While the DV quantum information can implement high fidelity task, the CV approach has the deterministic advantage of generation, manipulation and detection, and thus both of them are parallelly developed and the hybrid quantum information brings the hope of practical application. Single photon and entangled photons are the kernel resources and widely applied in DV quantum information tasks [39,40]. The squeezing is not only the important concept of quantum mechanics, but also the essential resources of quantum information technology [40–42]. Noise is unavoidable in quantum mechanics quantum, and squeezed state can significantly reduce quantum noise of one component to be below QNL while that of the other conjugate component is increased [43]. For entangled states, there are non-local quantum correlations between two sub-systems or among more sub-systems of entangled system [44]. The entangled optical modes can be generated by coupling squeezed optical modes on beam splitter (BS) and applied in quantum information protocols, such as quantum logical gates [45,46], quantum secret sharing [47–49], quantum teleportation [50,51], quantum entanglement swapping [45,52,53] and quantum interferometer [54]. Both the DV and CV quantum states have been widely employed in quantum information technology [40,55], and thus on demand storage and releasing of the DV and CV quantum states with high fidelity is a longstanding goal. So a variety of efforts have been done to store and release quantum states of optical modes. The EIT memory is suitable for non-classical optical modes, and quantum memories for single photon, squeezed and entangled states have been demonstrated based on EIT interaction [56–58]. QM for single photon polarization qubits with a fidelity of 99% has been demonstrated in balanced two channel laser cooled Rb atoms [39]. The DV polarization entangled

photon pairs have been stored in cold atom system. An input single photon is split into two orthogonally polarized on a beam displacer which forms the spatially separated entangled modes. These entangled photon pairs have been stored in two atomic ensembles and after a delay the entanglement is released onto photonic modes. The on-demand entanglement of two atomic ensembles has been generated by reversely mapping entangled states between photons and atomic spin waves [59]. Besides, the CV squeezed state resonant with Rb atomic absorption line can be generated by the optical parametric amplifiers (OPAs), and its squeezed quantum noise have been stored in cold and warm atoms [57,58]. Storing entanglement in quantum nodes and then releasing the stored entanglement from atomic ensembles to optical modes are the core problems for practical applications [60–62]. Two sideband modes of entangled states have been stored in two atomic ensembles based on QND interaction, which is used to create entanglement between two atomic ensembles [56]. With the development of quantum network, QM for multipartite CV entangled optical modes is required for the multiple users in quantum network, which can map quantum state between multiple entangled optical modes and quantum nodes in quantum network. EIT QM can map quantum state between the spatially separated CV entangled optical modes and atomic ensembles, which can deterministically entangle more atomic ensembles. Three entangled optical modes have been stored in three atomic ensembles and thus a GHZ-like state is mapped from spatially separated optical modes to distant atomic ensembles [63]. First, the tripartite GHZ-like entangled states are generated by coupling three squeezed states on an optical BS network. Based on the EIT interaction, tripartite entangled states are stored in three atomic ensembles. Lastly, the entanglement can be released from atomic ensembles into three optical modes on demand. QM for tripartite entangled states enables to entangle three atomic ensembles. According to the inseparability criterion for the tripartite CV entanglement, quantum memories for tripartite entangled optical modes and the tripartite CV GHZ-like entangled states of three atomic ensembles are verified. And QM for CV multipartite entangled states can be extended to entangle more atomic ensembles by storing CV entangled states with more optical modes. All the experiments have shown the EIT memory system has the capacity of keeping quantum nature [64].

This review discusses the recent developments in QM. We focus on EIT-based QM, including quantum memories implemented in warm atomic cell, cold atom and solid system, respectively. In addition, we review the state-of-the-art experimental developments on quantum storage and retrieval of non-classical optical modes, such as squeezed and entangled states. Particularly, we study the QM for tripartite entangled optical modes in three atomic ensembles.

## 2. The description of EIT

EIT is the result of quantum interference between atomic states caused by the interaction between coherent electromagnetic field and multi-level atomic system. Three possible structures of lambda($\Lambda$), ladder and vee-type(V) are in three-level system, as shown in Figure 1. $\Lambda$-type is applied in a wide range of QM because of its narrow bandwidth.

### 2.1. Theory of EIT

The $\Lambda$-type structure in Figure 2 involves a ground state $|g\rangle$, a meta-stable state $|m\rangle$ and an excited state $|e\rangle$. Two possible transitions can take place: one is a weak field between $|g\rangle$ and $|e\rangle$ as signal mode and the other is a strong field between $|m\rangle$ and $|e\rangle$ as control mode. When the two transitions enter the atom ensemble together, they will interfere destructively and lead the signal mode transparency [23,65,66].

The interaction Hamiltonian of light and atoms can be written as $\hat{H} = \hat{H}_0 + \hat{H}_{\text{int}}$, where $\hat{H}_0$ is the part of the bare atom, and the interaction $\hat{H}_{\text{int}}$ can be expressed as $\hat{\mu} \cdot \hat{E}$. Rabi frequency is $\Omega = \hat{\mu} \cdot \hat{E}_0/\hbar$, where $\hat{\mu}$ is an effective dipole moment, and $\hat{E}_0$ is the amplitude of electric field $\hat{E}$. $\Delta$ is the detuning of light frequency and transition. Considering that the detuning of signal and control are equal, $\Delta = \Delta_s = \Delta_c$. The Hamiltonian $\hat{H}_{\text{int}}$ of the three-level atom interact with a control laser of Rabi frequency $\Omega_c$ and a signal laser of Rabi frequency $\Omega_s$ in a rotating frame is [23]

$$\hat{H}_{\text{in}} = -\frac{\hbar}{2}\begin{bmatrix} 0 & 0 & \Omega_s \\ 0 & -2(\Delta - \Delta) & \Omega_c \\ \Omega_s & \Omega_c & -2\Delta \end{bmatrix} \tag{1}$$

The 'mixing angle' $\theta$ and $\varphi$ are used to simplify the Hamiltonian result,

$$\begin{aligned} \tan\theta &= \tfrac{\Omega_s}{\Omega_c} \\ \tan 2\varphi &= \tfrac{\sqrt{\Omega_s^2+\Omega_c^2}}{\Delta} \end{aligned} \tag{2}$$

The atomic state will convert to a zero energy state and a pair of components of the atomic states with energy $\frac{\hbar}{2}\left(\Delta \pm \sqrt{\Delta^2 + \Omega_s^2 + \Omega_c^2}\right)$. The eigenstates can be expressed as

$$\begin{aligned} \left|\hat{a}^+\right\rangle &= \sin\theta\sin\varphi|g\rangle + \cos\varphi|e\rangle + \cos\theta\sin\varphi|m\rangle \\ \left|\hat{a}^0\right\rangle &= \cos\theta|g\rangle - \sin\theta|m\rangle \\ \left|\hat{a}^-\right\rangle &= \sin\theta\cos\varphi|g\rangle - \sin\varphi|e\rangle + \cos\theta\cos\varphi|m\rangle \end{aligned} \tag{3}$$

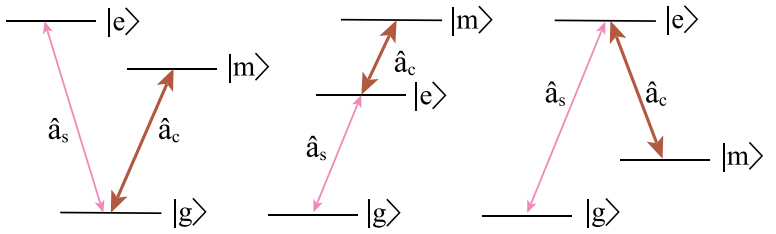


**Figure 1.** The vee-type (V), ladder and lambda ($\Lambda$) structures in three-level system.

If the signal mode is weak ($sin\ \theta = 0$), and the signal mode is on resonance ($tan\ \varphi = 0$), and thus the dressed states will form in the usual condition. Within an adiabatic process, the Rabi frequency changes from $\Omega_s \ll \Omega_c$ to $\Omega_c \ll \Omega_s$ with gradual increasing $\Omega_s$ and decreasing $\Omega_c$. The initial state $|\hat{a}^0\rangle = |g\rangle$ will evolve into a meta state $|m\rangle$, which forms a dark state.

The EIT dynamics process depends on the master equation $\dot{\hat{\rho}} = [\hat{H}, \hat{\rho}] - \gamma\hat{\rho}$, where $\gamma$ is coherent relaxation rate. Linear susceptibility $\chi$ satisfies the equation $\hat{P} = \varepsilon_0\chi\hat{E}$ in EIT [67]. The real part of $\chi$ describes dispersion, and the image part describes absorption. The detuning directly influences the windows of EIT. When detuning is zero, signal mode and control mode are on resonant, and the strength of interaction $g$ is maximum. The linear susceptibility can be written as [65].

$$\chi = -\frac{g^2 N(\gamma_{gs} + i\Delta)}{(\gamma_{ge} + i\Delta)(\gamma_{gs} + i\Delta) + \Omega_c^2} \tag{4}$$

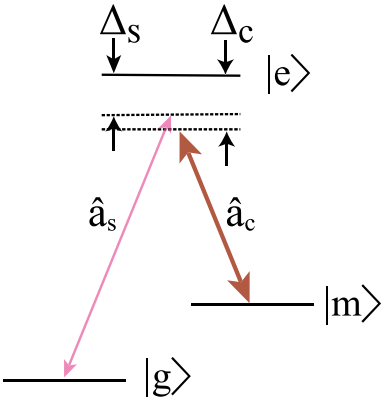


**Figure 2.** The general EIT system.

where $N$ is the number of atoms and $\gamma_{ij}$ is the decay rate from energy level j to i. Then the amplitude transfer T can be obtained from the function $T = \exp\{-kIm(\chi)L\}$, where $k = 2\pi/\lambda$ is the wave number and L is the length of medium. Then the transparency width can be calculated by the atoms number density and the absorption cross section [65].

Another important character in EIT is 'slow light'. The velocity is related to refractive index within the real part of $\chi$, as well as the phase velocity and the group velocity can be expressed by the refractive index $n$ in equation

$$v_{\mathrm{p}} = \frac{c}{n}, \quad v_{\mathrm{g}} = \frac{c}{n + \omega\frac{\partial n}{\partial \omega}}, \quad n = \sqrt{(1 + Re(\chi))} \tag{5}$$

Harris SE, et al. first have pointed out the group velocity of light could be slowed down with EIT [68], then Kasapi A, et al. have realized the group velocity of 165 times degraded in pure lead vapor [69]. In the remarkable work, Hau L, et al. have slowed the signal mode to 17 m/s in the ultracold Na atoms [70]. Besides, the slow group velocity in warm atomic vapor has been achieved in the same level [71,72].

### 2.2. Dark-state polaritons

Dark-state polaritons have been proposed by Fleischhauer M, et al. [25,32], where there exists a quasiparticle and results in the slow group velocity in EIT. The quasiparticle consists of a mixture of electromagnetic field $\hat{E}$ and spin waves $\hat{\sigma}_{gm}$, the information from photon converts to spin wave polariton by changing the control mode. The quantum state completely transforms to spin wave in an adiabatic process, when the control mode is turned off. With the weak signal mode and the strong control mode, the evolution propagation equation of the electric field can be written as [70]

$$\left(\frac{\partial}{\partial t} + c\frac{\partial}{\partial z}\right)\hat{E}(z,t) = igN\hat{\sigma}_{ge}(z,t) \tag{6}$$

The atoms are populated at $|g\rangle$ in $\hat{\sigma}_{gg} = 1$. The control mode is varied slowly so that it does not influence the cross length of the signal mode. Considering a time varied control mode, the electric field and spin wave can lead to a new quantum quasiparticle, which are given by

$$\hat{\Psi}(z,t) = \cos\phi(t)\hat{E}(z,t) - \sin\phi(t)\sqrt{N}\hat{\sigma}_{gm}(z,t) \tag{7}$$

$$\cos\phi = \frac{\Omega}{g^2N + \Omega^2}, \sin\phi = \frac{g\sqrt{N}}{g^2N + \Omega^2} \tag{8}$$

The dark-state polaritons theory gives evolution of quantum states between light and spin waves. Three stages of compression, storage and releasing of optical pulse in memory medium are necessary for implementing QM. The propagation of a dark-state polariton in Figure 3 shows quantum state transfer in QM in three stages. The mixing angle is rated and shown in (a). The coherent amplitude of the polariton, light and matter components are plotted in (b), (c) and (d), respectively. From (c) and (d), it can be seen that the quantum state is transferred between light and matter. In the compressed process $(-\infty < t < 0)$: when signal and control mode interact with atomic ensemble simultaneously, the signal mode is compressed into the atomic ensemble, and the dark-state polaritons are generated in this process $\hat{H}(t) = \hat{H}_{\text{int}}$. Next process is the storage process $(0 < \text{t} < \text{T})$, when the signal mode is totally compressed into the atomic ensemble, the control mode is switched off. At the storage time T, the quantum state is stored into atomic ensemble, in this process $\hat{H}(t) = 0$. Last process is the released process $(\text{T} < \text{t} < \infty)$: when the control mode is switched on again, the quantum state is transferred from atomic ensemble and the signal mode is released, in this process $\hat{H}(t) = \hat{H}_{\text{int}}(\Omega_p = 0)$.

## 3. Quantum memory for classical state

There are many different memory mediums based on EIT, some of which are discussed in this section. The different characters of atoms with the good coherence promote the development of QM. Some crucial properties including memory efficiency, fidelity, memory lifetime and bandwidth are vitally important to evaluate the system. The memory efficiency is obtained by the photon number ratio between the output and input mode. Fidelity describes the overlap of the input state and released state and is an only way to estimate the memory performance. High-fidelity optical QM faces some difficulties for practical applications, mainly due to the quantum de-coherence. The fidelity is limited by memory efficiency and memory noise. Thus, high efficiency and low noise QM are demanded for practical applications. On the one hand, the improvement of memory efficiency is essential, which has been implemented by means of large optical depth [73]. On the other hand, the suppression of FWM noise, which is the main memory noise, is the key for high fidelity QM. Under conditions of EIT accompanied by a process of FWM, quantum noise can be suppressed by using interference destruction of optical cavity [31] or preparing the signal and idler modes in a two-mode squeezed vacuum state [74]. Besides, the long memory lifetime is the key parameter of QM and ensures the good coherence for quantum repeater [30].

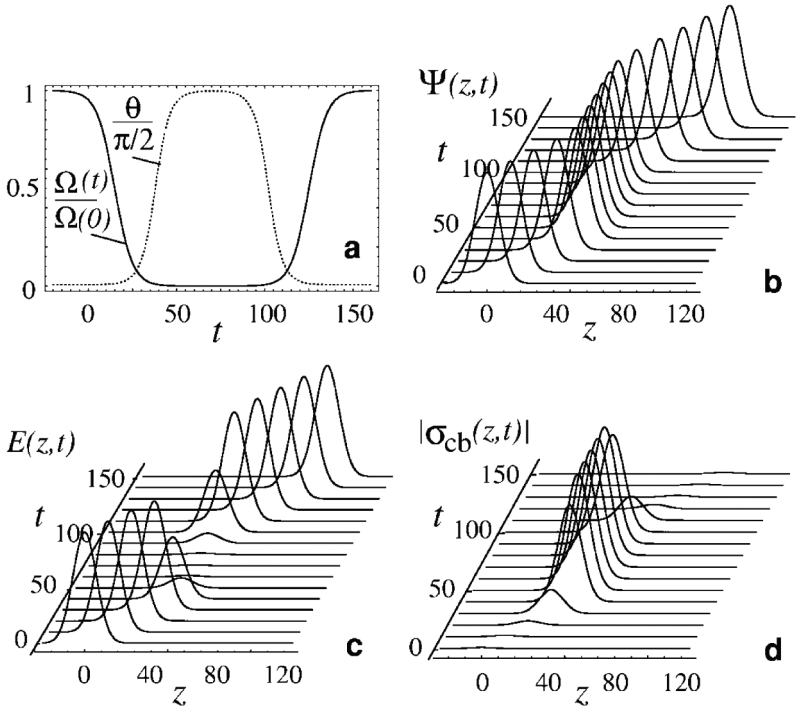


**Figure 3.** Propagation of a dark-state polariton. (a) The mixing angle is rotated from 0 to $\pi/2$. (b) The coherent amplitude of the polariton, light and matter components are plotted. (c) (d) the quantum state is transferred between light and matter, respectively. Reprinted with permission [32].

The warm atomic ensemble, cold atomic ensemble, solid state and so on can be implemented in QM. In general atomic EIT, high efficiency of photon memory in atomic system has been achieved by using controlled wave shapes for the control field [75]. Later, QM of single-photon polarization qubits can be implemented via double EIT, where the optimal optical depth can be given for both maximum efficiency and high fidelity by suppressing the optical absorption and dispersion via the optimal input qubit pulse and the amplitude of the control field [76]. A cold Rydberg atomic gas can be used as one of ideal memory platform. Photons have been stored with fast quantum state generation and long lifetime [77,78]. Moreover, the nonclassical storage and retrieval of a multiphoton pulse has been realized [79]. A stable high-dimensional single light bullets and vortices have been generated, stored and retrieved with high efficiency and fidelity [80]. Besides, in quantum dots with a Rashba spin-orbit coupling, a highly efficient and controllable storage and routing of single photon have been realized [81].

The linear probe pulse suffers serious distortion for retrieved pulse, because the dispersion in EIT leads to the spreading and attenuation. Starting from derive a nonlinear Schrodinger equation describing the

evolution of the probe-field envelope, optical solitons with an ultraslow propagating velocity and extremely low generation power can be obtained. Besides linear optical pulses, EIT can be used for the memory for nonlinear optical pulses. QM for a stable nonlinear optical pulse can be realized in an ultracold ladder-type three-level atomic gas [82]. The storage and retrieval of optical soliton can be realized in a coherent atomic system [83,84]. The memory for a surface polariton can be realized in quantum emitters doped at the interface between a dielectric and a metamaterial [85].

### 3.1. Quantum memory in warm atomic ensemble

Warm vapor is more convenient and scalable compared with cold atoms, because its OD can be enlarged by increasing the temperature, and its coherence time can be improved by the paraffin coating. The memory efficiency mainly depends on OD [73]. In order to improve the efficiency, the different temporal function of input pulse can be used. For a given system, the optimal temporal function of signal mode is determined under a given OD by iteration method, which realizes the high memory efficiency.

Novikova I, et al. have mentioned and proved the iteration method in 2007 [35], which can apply in both classical and quantum regimes. In a 7.5 cm vapor filled with $^{87}$ Rb and 40 Torr Ne, the temperature is 60 ° C and the OD is 9. A three layers magnetic shield is used to prolong the coherence time of Rb atoms. The beam from laser is divided into two sections: one beam is shifted 6.8 GHz by electro-optical (EOM) as the control mode, and the other directly is used as the signal mode corresponding to D1 transition of $^{87}$ Rb. The wavelengths in atomic system are usually 780 nm (795 nm) and 852 nm (895 nm) which correspond to the D2 (D1) absorption lines of Rb and Cs, respectively. The D1 transition is simple in EIT because other energy level is far from this line. The optimal input temporal function is gotten by iterating the released mode shape as input until the input and output pulse shapes are similar. Figure 4 shows the iteration signal mode by a certain control mode and the efficiency with different pulse shape. One to five are the number of each iterative experiment, and its efficiency grows in each experiment until the input signal mode shape becomes optimal. It is based on an assumption that the control mode shape does not influence the efficiency in each experiment [86]. The OD and the Rabi frequency of the control mode are the main factors. So the process of finding the optimal pulse means a mutual matching pair of control and signal modes to the spin wave of the atoms. Its dynamic equation is described as [73]: the time from -$\infty$ to 0 represents the input mode shape, and the output mode describes from T to $\infty$ after storge time T. $\hat{P}$ represents optical polarization operator from the ground state to the excited state. $\hat{S}$ is spin operator. $\gamma_s$ is the decay rate of spin wave, which directly relates to the

lifetime of the memory. Considering adiabatically approximation, eliminating $\hat{P}$ simplifies the system. Another important parameter is interaction coefficient $g\sqrt{N}$. The experiment results are constant with the theory prediction and realize above 40% memory efficiency. In some special cases, the input pulse shape is fixed, so the shape cannot be modulated by EOM or acousto-optical modulators (AOM). For a given signal mode shape, the efficiency also could be improved by modulating the control mode shape. A possible way is provided to calculate the control mode shape [87]. Such the control mode shape is used to map the signal mode onto the true spin wave. Therefore, it is verified that the maximum efficiency always can be obtained under a given OD by using the optimal signal or control mode shape independently.

### 3.2. Quantum memory in cold atomic ensemble

QM in cold atom based on EIT is explored recently. The cold atomic cloud is collected by the magneto-optical-trap (MOT) as memory medium to store classical coherent optical state. In cold atomic QM, where a cold-atom cloud is generated by applying a moderate extra magnetic field in the MOT, and QM with high memory efficiency, high fidelity and long lifetime has been demonstrated.

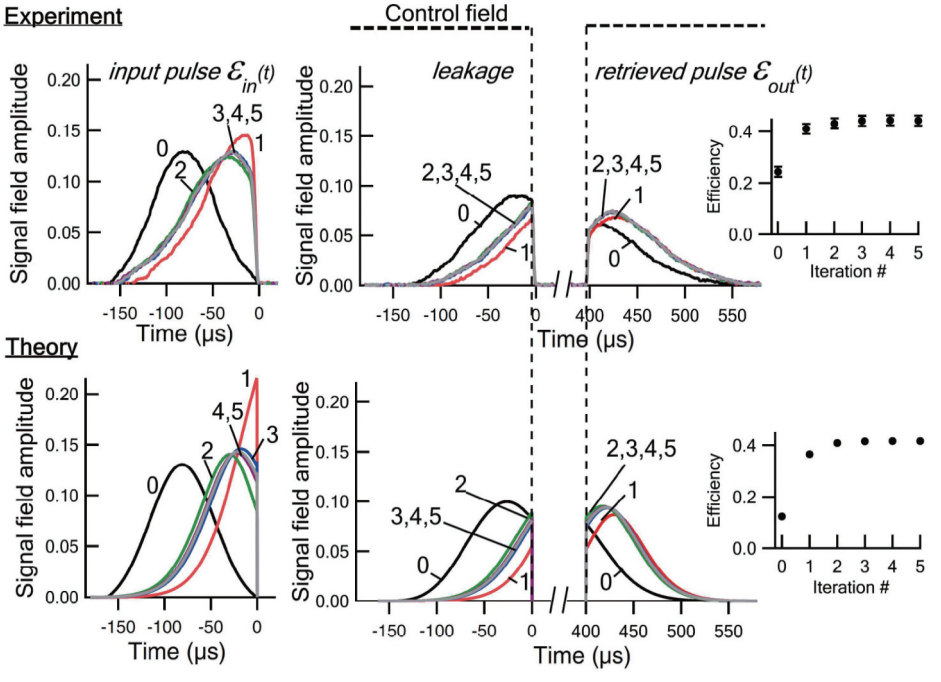


**Figure 4.** The iteration signal mode by a certain control mode and the efficiency with different pulse shape. Reprinted with permission [35].

The initial state $|g\rangle$ needs to be prepared by pumping the whole population and trapping the atoms ensemble for a while to increase the atomic density and OD of the system. Chen YH, et al. have achieved the slow group velocity and light storage by cooling the $^{87}$ Rb atoms ensemble to around 300$\mu$K in a magnetic optical trap [88]. The signal mode $\Omega_p{}^{\pm}$ is injected along the major direction of the atom cloud. The control mode contains light toward and backward with an angle of $0.4^{\circ}$ along the signal mode. Figure 5 is the experiment setup for QM in cold atoms and the energy level. $\Omega_p$ and $\Omega_c$ are the Rabi frequencies of signal and control modes respectively, and the OD has reached 156 in this condition. Photon detectors PD1 and PD2 are used to collect the signal photons in forward and backward with collection efficiencies of 52% and 68%, respectively. Finally, the memory efficiency of 78% is achieved by using a 1.5 $\mu$s Gaussian pulse, and its coherence time is 98 $\mu$s. After this study, high fidelity and long memory lifetime have been achieved by lifting Zeeman degeneracy [89]. First of all, a pair of orthonormal bases are needed to store polarization qubit act on atoms. The signal and control modes enter along the quantum axis of atoms, which can decrease the decoherence. In a weak magnetic field, four energy structure can be simplified as three energy levels. Such process of storage is described by dark state. During shutting off the control mode adiabatically, the information is stored in a superposition state. In cold atom mechanism, memory time mostly depends on the atoms motion, where $t_d = 1.3r_0/v_r$, $r_0$ is the radius of signal mode, and $v_r$ is the average atom velocity ($v_r = \sqrt{2k_bT/m}$). When the control pulse is turned on, the spin wave is mapped onto signal mode. Finally, the high fidelity is achieved, and the fidelity has been varied from 98.6% with 200 $\mu$s to 78.4% with 4.5 ms memory time.

Cs atoms contribute to the minimal four wave mixing (FWM) effect due to its lager ratio of the hyperfine splitting to the spontaneous decay. The decoherence can be optimal through reducing the angle between the control and signal modes, because the slight phase mismatching can destroy the matching condition to reduce noise. In a low noise condition, the overall efficiency depends on the slow light and the dark state polariton. For shorter memory time and larger OD, the maximum overall efficiency finally gets close to the transmission efficiency. The overall efficiency is divided into three parts including transmission, compression and releasing, which is analyzed on Maxwell-Bloch equation [36]. In experiment Hsiao YF, et al. optimize a cold atomic Cs trap to realize QM. With the 20 ns signal pulse and $\Omega_c = 24\Gamma$, the OD ups to 1000 and the optimized waveform of signal mode are used in experiment. The next part introduces the optimized signal mode. Because the FWM is increased with the OD, the fidelity is inverse to the FWM gain [90]. The efficiency reaches 92% and its FWM gain is $<$ 3% when OD is selected to 816 for reducing noise.

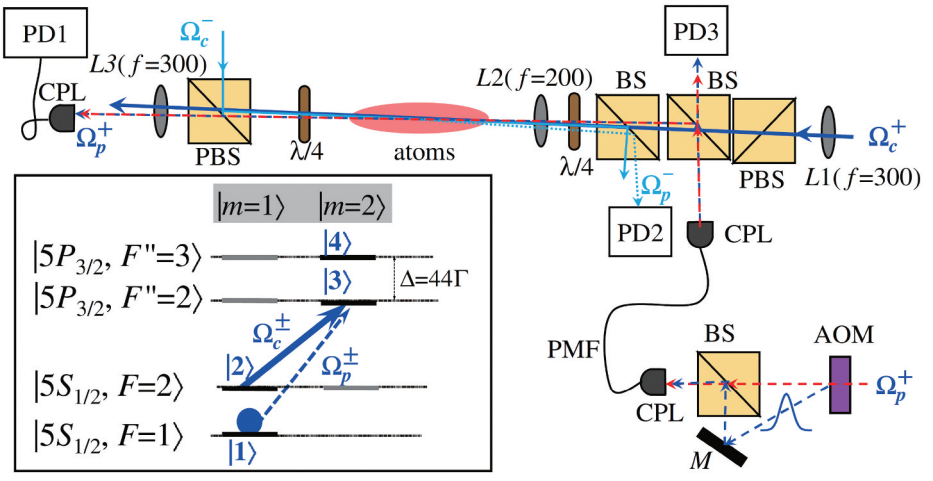


**Figure 5.** The experiment setup for QM in cold atoms. The energy level shows in the bottom left. Reprinted with permission [88].

In this year, a spatial dual-rail memory has been realized at the single photon level, besides dual-rail details describe elaborately in single-photon state section. The polarization state of 68% memory efficiency and 99% fidelity have been achieved with an OD around 200 [37]. So the multiplexing approach provides one way to realize high-capacity QM.

### 3.3. Quantum memory in solid state

Solid state not only has long coherence time but also can be extended to other wavelength with the rare earth ions. Broad bandwidth is used in a wide range of application [38,91–93]. Therefore QM in the rare earth ions becomes one of the valuable methods. For the rare earth ion of solid, the energy in 5s or 5p shell is smaller than 4f shell in the farthest electronic shell of rare earth ions, so the electron will fill the 5s and 5p shell first. In this way, the electrons in 4f will be isolated by two layers shell, and it leads to the narrow bandwidth and longer coherence time. The lifetime of spin wave can be prolonged by adding the external magnetic field. The spin echo can be used to overcome the fast decay of spin inhomogeneous broadening.

Heinze G, et al. have realized a long lifetime memory in 2013 by combining EIT and zero first order Zeeman point [94]. The intensity and frequency are adjusted by the evolutionary algorithm to realize the optimized memory efficiency, and the magnetic field is also optimized in the experiment. In the $Pr^{3+}$:$Y_2SiO_5$ crystal, the image information of 605.98 nm signal fields is stored into atomic coherences by using EIT mechanics. Through preparing the initial state, the signal mode converts to the atomic coherence. After memory time T, the control mode destroys the atomic coherence and gets the retrieval signal

mode. The signal amplitude is measured by photo-electric detector, and the memory time has reached up to one minute. Figure 6 shows the signal mode energy and the retrieved images vary with memory time. Because memory efficiency mainly depends on OD, the simply way is increasing the density of ions or the length of the crystal to increase OD. However, the density and length usually are determined by the growth of the crystal. If the crystal is a few millimeters, its OD is under 10. Another useful way is multi-passing through the crystal, which remarkably increases the length of interaction with through times M. Though the crystal length is small, it still could realize a stronger interaction. So, the muti-pass configuration reduces the need of crystal in QM. In 2016, Schraft D, et al. set up a multi-pass configuration in a rare-earth ion-doped crystal. The OD can increase 16 times from 6 to 96, and a high efficiency up to 76.3% is achieved [38]. The multi-pass could be set up by pairs of lenses, and the signal mode moves in a small displacement by adjusting an optical mirror, but the beam position through the crystal is fixed each time. After several transmission times, the displacement of signal beam is out of the mirror and it has already achieved M passes. The times will double if the signal mode is reflected and traveled another same distance out of the system, and thus 2 M passes are realized. The control mode reverses through the crystal propagation axis with an angle of 1°. With lager OD, the more signal modes are compressed in the crystal. The efficiency is improved from 33.8% for single pass to 67% for 10 passes. The optimal waveform is also verified in the experiment with a maximal memory efficiency of 76.3% for 14 passes.

## 4. Quantum memory for non-classical states

The non-classical states of light are widely applied in quantum information science, and thus QM for the non-classical states of light is demanded. In general, non-classical states include single-photon state, squeezed state and entangled states. The non-classical states of light are the important quantum resources for quantum information, and very fragile due to the unavoidable decoherence. Thus, QM for non-classical states of light is critical for both high memory efficiency and memory noise close to quantum noise limit, which ensures a high-fidelity QM. QM of non-classical states can be applied in quantum information processes, such as quantum computation, quantum measurement and quantum clock network.

### *4.1. Quantum memory for single-photon state*

DV QM with higher fidelity has practical applications in quantum information processing and quantum computation. As well known, in a QM processing, higher memory efficiency and higher fidelity are essential for QM. For example, linear optics quantum computation requires the

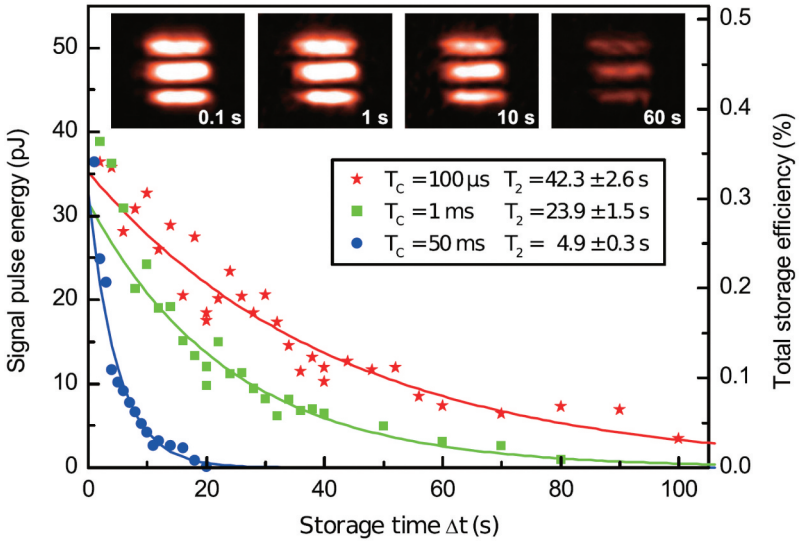


**Figure 6.** The signal mode energy and the retrieved images varies with memory time. Reprinted with permission [94].

manipulation of single-photon qubits and cannot work with coherent light pulses [95]. So many groups dedicate to the research of QM for single photon. Wang YF, et al. have been achieved the high-performance single-photon QM, based on two-channel EIT in laser-cooled $^{85}$ Rb atoms [39,96]. To realize efficient single-photon QM, there are two main challenges to be tackled. One of them is suppressing the extra noise. Extra noise is unavoidable in practical experiment and significantly degrades the fidelity of a single-photon state. By setting an angle between the control modes and the signal modes, the scattering and coupling of the control modes to the signal modes have been suppressed, and by combing with other efficient filtering techniques, low noise and high single-photon purity are achieved. Besides, the FWM noise is significantly suppressed by the phase mismatching due to the large angle separation in nonlinear process [97]. The other challenge is taking advantage of single-photon with controllable spectral-temporal states to match the signal modes. The primary approach is photon shaping technique. The Gaussian-shape biphoton waveform is generated by mapping the pump field spatial profile onto the atomic cloud. Solving these two problems is the key to complete the experiment. The experimental setup and energy level scheme of the single-photon QM are shown in Figure 7. The atomic energy level scheme of the QM based on EIT is $\Lambda$-type three-level system. There are double MOTs of cold $^{85}$ Rb atoms in experiment. The heralded single-photon source is generated firstly, and the QM process is operated secondly. In the first MOT $_1$, the time-frequency entangled narrow-band paired Stokes and anti-Stokes photons are generated by spontaneously mapping counter-

propagating pump and coupling beams to atomic cloud. When a Stokes photon is detected, its paired frequency anti-correlated anti-Stokes photon is projected to a pure single-photon state with a temporal waveform to match the signal modes [98,99]. The generated anti-Stokes photons with optimal Gaussian-shape are circularly polarized. After passing through a quarter wave plate (QWP) and a polarization-maintaining single-mode fiber, an arbitrary polarization state $\hat{S} = \cos\frac{\alpha}{2}|H\rangle + e^{i\beta}\sin\frac{\alpha}{2}|V\rangle$ is created, where $\alpha$ and $\beta$ are the angles denoting the polarization state on the Bloch sphere, and $|H\rangle$ and $|V\rangle$ are the two polarization bases. The polarization modes are spatially separated after a beam displacer (BD). Then the single-photon enters the second MOT $_2$ [96], and the control laser beam is switched off. During the storage time, the single-photon is stored and preserved in atom medium. Then the control laser beam is switched on to release the photon modes from input modes. It is worth noting that storing the polarization qubit state in the two-dimensional Hilbert space, a spatially multiplexed dual-rail scheme is utilized to convert the two polarization bases into two spatial modes. The two released modes are combined after the BD, and detected simultaneously by a polarization qubit analyzer. Besides, the two spatial channels are required to have identical memory performance to achieve high fidelity. By measuring the released modes, a single-photon polarization qubit memory efficiency and fidelity can reach 90.6% and 99%, respectively. In addition, the fidelity will decrease with longer storage time because of the reduced memory efficiency and the increased two-photon probability. The two-channel QM configuration with high memory efficiency and high fidelity can push the photonic QM closer to practical applications in quantum network.

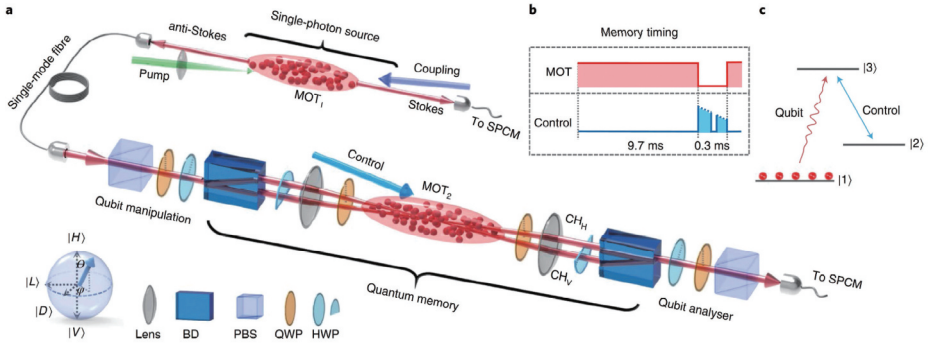


**Figure 7.** Experimental setup and energy level scheme of the single-photon QM. (a) Schematic of the experimental optical setup. (b) The memory operation timing shows the MOT sequence and the optimized control laser intensity time-varying profile in each experimental cycle. (c) The atomic energy level scheme of the QM based on EIT. Reprinted with permission [39].

### 4.2. Quantum memory for squeezed states memory

QM for squeezed states of light is a necessary component of quantum information science and technology that will significantly improve the precision of quantum measurement [57,58]. So the storage and retrieval of squeezed states of light are necessary in actual application.

In the QM for squeezed state of light based on EIT system, the first step is preparing squeezed light. The experimental setup for generation, storage, and transfer of squeezed state is shown in Figure 8 [58]. A Ti: Sapphire laser pumped by a single frequency solid state laser is tuned to the $^{87}$ Rb transition at 795 nm, which is used as the fundamental wave laser of the second harmonic generation (SHG). Then the resulting second harmonic light pumps our squeezed light source, a degenerate optical parametric amplifier (DOPA) [100], which produces the squeezed light. To store the squeezed light, the DOPA output squeezed light has to be chopped into microsecond pulses by an ultrafast mechanical chopper to decrease the optical losses. The EIT control light frequency shift of 6.8 GHz is provided by a separate diode laser. The squeezed light has entered into atomic ensemble and been retrieved after a period of storage time, and finally the memory efficiency is measured by the photon detector. Due to the unavoidable excess noises in the experiment, the noise values of the measured released states are always higher than the shot noise. The quadrature components for the input and released signal light are measured by means of balanced homodyne detector (BHD) with a local oscillator (LO) derived from the master oscillator. The quadrature noise of signal mode can be analyzed by employing the time-domain method, which acquires the signal from the detector and performs Fourier transform of the obtained real-time waveform [101–104]. In this measurement, $S(\vartheta)$ represents the measured power noise, where $\vartheta$ is the phase difference between the squeezed state and the LO, $\vartheta = 0$ and $\vartheta = \pi/2$ stand for maximized and minimized noise value, respectively. The relative phase is controlled and locked by means of Pound-Drever-Hall technique. By combining with adjusting the sampling rate of real-time homodyne signal and averaging the trials of Fourier-transformed power noise, the varied noise spectra of the squeezed state are obtained. In recent study, 600 ns pulse of 1.86 dB squeezed state at 795 nm has been stored in a Rb cell, and the released pulse of 0.21 dB is analyzed by homodyne tomography [57]. The squeezed state pulse with a temporal width of 930 ns has been stored in laser cooled Rb atoms, and the squeezed state of 0.16 dB has been released at the storage time of 3$\mu$s [58]. It is worth noting that when the squeezed state is stored in the atomic ensemble, the collective atomic spins are also squeezed, and their quantum fluctuation is suppressed below the shot noise.

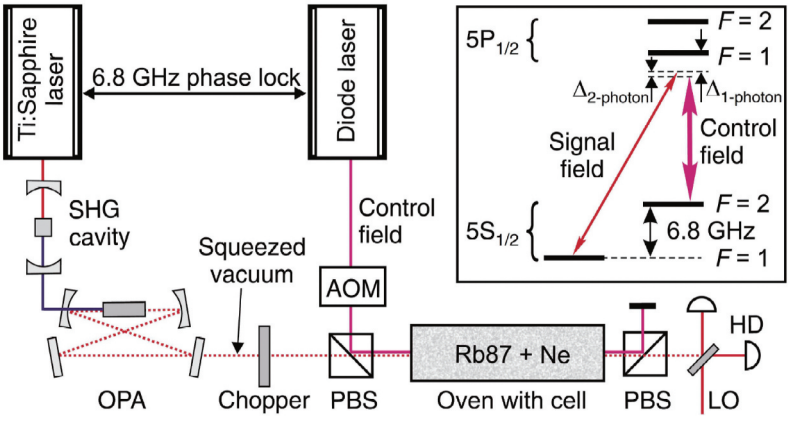


**Figure 8.** Experimental setup. the inset shows the atomic level configuration. Reprinted with permission [57].

### 4.3. Quantum memory for entangled states memory

In quantum network, quantum repeater architecture is essential and could efficiently overcome transmission loss to achieve long-distance information transmission. In 2001, Duan, Lukin, Cirac and Zoller proposed an original approach to perform scalable long-distance quantum communications, involved atomic ensembles, linear optics and single photon detectors. Storing and distributing entanglement among distant matter nodes by means of photonic channels are the fundamental portion. Generally atomic ensembles can play the role of such nodes [20]. Quantum information of entanglement is able to map onto atomic ensembles by QM.

#### 4.3.1. Quantum memory for entangled photons memory

Quantum state transferred from DV entangled states of light to atomic spin waves is an effective approach. QM for entanglement enables to entangle two atomic ensembles which has been proved based on EIT by Kimble HJ [62]. The experimental setup is depicted in Figure 9. In order to separate the generation of entanglement and its storage, a single photon is split and performed [105–107]. After the entangled photons are mapped into atomic ensembles, the stored entanglement is mapped back into photonic modes. Then the released entanglement is distributed into two remote atomic ensembles for quantum network. The progress mainly concludes two procedures [108]. The first stage is entanglement swapping, single photons are polarized at 45° from the eigen-polarizations of the beam displacer, which are split into two photon modes to generate an entangled state of light. The next stage is that the entanglement is coherently mapped onto two spatial cold

atomic ensembles in MOT to create the entanglement between two ensembles. The spin-polarized atomic ensemble into one Zeeman sublevel of a hyperfine ground state is used to avoid dissipation for the necessary polarization of photon modes in this process. This mapping leads to heralded entanglement between two ensembles. After user-controlled time, the stored atomic entanglement is converted back into entangled photonic modes to transmit. By using the fitted function of the input signal mode as the initial condition with all other parameters, an overall memory efficiency can be obtained, which is in agreement with the simulation of theory [32]. Released entanglement is measured by constructing the reduced density matrix. The QM efficiency is concluded in the total transmission efficiency of entanglement from input modes to output modes. Optimal pulse shaping and OD are adopted, and the entanglement transfer efficiency could be greatly improved. The presence of entanglement between the two atomic ensembles is explicitly quantified. Therefore QM of entanglement is vital in quantum information, and entanglement could be significantly preserved by atomic nodes.

### 4.3.2. Quantum memory for tripartite entangled states memory

Besides QM for entangled photons, the on-demand storage and release of CV entangled states of light are demanding. In the regime of CV, a notable advance has been used to transfer quantum states between light and matter. Quantum networks must have the crucial ability to entangle quantum nodes. QM of multipartite entanglement based on EIT is verified [63]. The experimental setup for generation, storage,

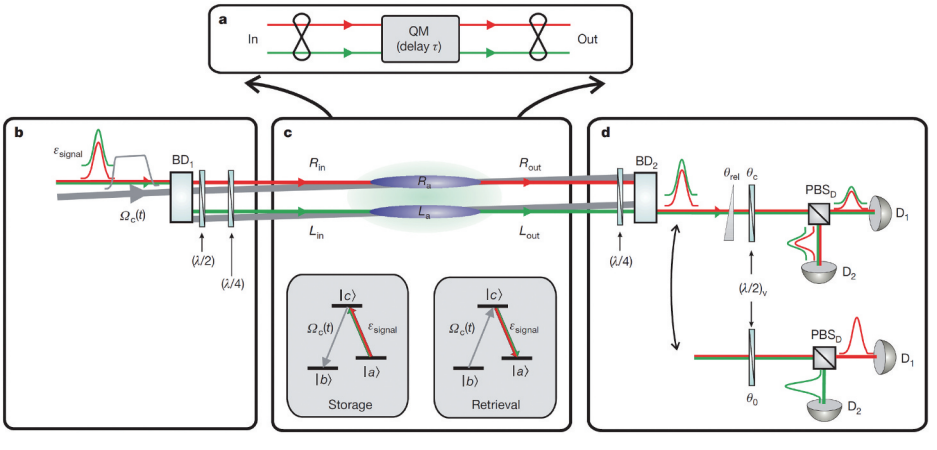


**Figure 9.** (a) Reversible mapping. Illustration of the mapping of an entangled state of light into and out of a QM. (b) Entangled a pair of photons. (c) Quantum interface for reversible mapping. (d)Entanglement verification system. Reprinted with permission [59]

and transfer of tripartite entanglement is described in Figure 10. At first, the tripartite optical entangled states is off-line prepared (part I). A Ti:Sapphire laser is used as the fundamental wave laser of the SHG, and input seed laser to pump the three DOPAs, which produce three squeezed vacuum states. The squeezed states are coupled at two optical BSs to generate three narrow band entangled optical beams turned to the transition of Rb D1 absorption. Quadrature phase squeezed state is generated by OPA1 that operates at the parametric amplification, and the quadrature amplitude squeezed states are generated by OPA2(3) that operates at the parametric de-amplification. The output optical fields from OPA1 and OPA2 are coupled at a 1:2 optical BS, and then the output optical modes from this BS and OPA3 are coupled at a 1:1 BS. Then the tripartite entanglements are stored into three atomic ensembles and the preserved entanglement is subsequently transferred back into optical entangled states (part II). In this process, the tripartite entangled states pass through three pairs AOMs to shape wave packet and the control laser passes through a high speed EOM to achieve frequency shift. At last, the three released entangled states are measured by three BHDs (part III). The released entanglements pass through the Glan–Thompson polarizers and a series of etalons to filter control laser. Only the entanglement reached three sets of BHDs is measured combining with LO from Ti:Sapphire laser. The criterion of quantum correlation variances is used to estimate whether there is an entanglement among three atomic ensembles [109]. The correlation variances can be obtained by measuring the quadrature amplitudes and quadrature phases of input and released signal modes with the help of BHDs [110–112]. When the gain factors are took the optimization to minimize the corresponding correlation variances, the sum of correlation variances for three released signal modes is less than 1 [62]. The entanglement among released signal modes is verified by criterion inequalities. The value in experiment is consistent with the calculated result in theory. Thus, the tripartite GHZ-like entanglement among three space-separated atomic ensembles is experimentally demonstrated and this system has the capacity to preserve multipartite entanglement. Overall, the performance of QM for tripartite entangled states memory is mainly limited by the quality of entanglement source and the fidelity of memory system. The QM for multipartite entangled states is the foundation of Quantum information. For example, the QM for multipartite entangled optical modes can be potentially applied in distributed quantum logic gates. If the fidelity of QM is high enough and good quality of multipartite cluster state resource is employed, it is possible to realize distributed quantum logic gates.

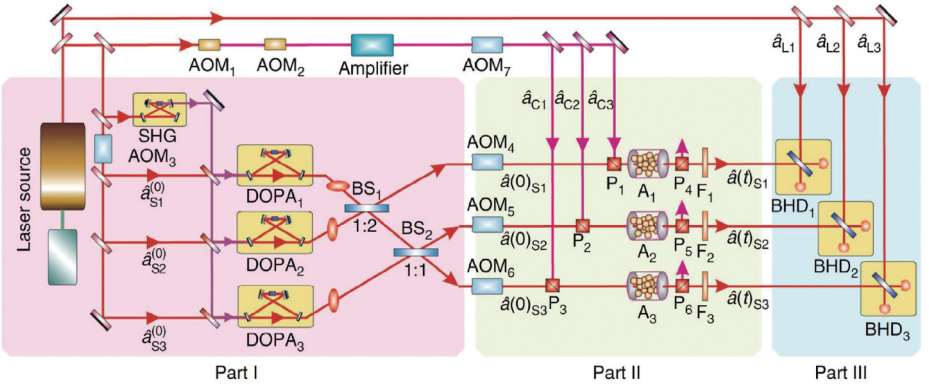


**Figure 10.** Schematic diagram. Experimental setup. It includes three parts, Part I is the generation system of tripartite optical entanglement; Part II is the transportation of tripartite entanglement to three distant atomic ensembles; Part III is the entanglement verification system. Reprinted with permission [63].

## 5. Conclusions and Outlook

In summary, we have reviewed the developments in the past few years of EIT-based QM in the warm and cold atomic ensembles and solid system, respectively, which is the building block of quantum network. The EIT interaction between light and atoms enables to store and release optical modes. Quantum memories for non-classical states of optical modes are necessary for establishing and storing non-classical states of light in atomic ensemble. Especially, tripartite entangled states of optical modes can be generated by means of three OPAs and the BS network, and the quantum memories for non-classical states including squeezed state and entangled states have been proved. The multipartite entangled states can be generated by storing multipartite entangled optical modes.

High-performance QM is demanding for practical applications, and there are many techniques which enable to improve the performance of QM. Because the optical cavity can enhance the light–-atom interaction, the conversion efficiency of atomic spin wave to photons can be increased [113,114]. Besides enhancing the memory efficiency, the cavity can effectively suppress the memory noise. The paraffin coating of the warm atom cell wall can extend the memory lifetime, and in this way the lifetime can reach the scale of millisecond [22,56]. Quantum entanglement of remote quantum nodes holds promise for the applications of quantum network. Quantum frequency conversion enables to shift between atom and telecommunication wavelengths to greatly extend the distance of entangled nodes. High-performance QM can advance the high-fidelity quantum information processing. There are many interesting topics to study in the practical applications of these high-quality quantum memories such as distributed quantum

gates [21] and quantum enhanced atomic magnetometry [22]. Atomic ensemble based QM enables to implement distributed quantum computation and quantum enhanced atomic magnetometry [22,115]. The distributed controlled-phase gates can be implemented by storing quadripartite cluster-like optical modes, which is the essential integral of one-way quantum computation [115]. Spin squeezing can be generated by storing squeezed state and enables the sub-QNL sensitivity of magnetometry [22,116].

## Disclosure statement

No potential conflict of interest was reported by the author(s).

## Funding

The authors thank Luis A. Orozco for his helpful discussion. This research was supported by the National Natural Science Foundation of China (Grants No. 62122044, No. 61925503, No. 11904218, No. 12147215, No. 61775127 and No. 11834010), the Key Project of the National Key R&D program of China (Grant No. 2016YFA0301402), the Program for the Innovative Talents of Higher Education Institutions of Shanxi, the Program for the Outstanding Innovative Teams of Higher Learning Institutions of Shanxi and the fund for Shanxi ' 1331 Project' Key Subjects Construction.

## ORCID

Zhihui Yan http://orcid.org/0000-0002-7149-4939
Xiaojun Jia http://orcid.org/0000-0001-5499-5427

## References

[1] Yin J, Cao Y, Li YH, et al. Satellite-based entanglement distribution over 1200 kilometers. Science. 2017;356:1140–1144.
[2] Huo MR, Qin JL, Cheng JL, et al. Deterministic quantum teleportation through fiber channels. Sci Adv. 2018;4:eaas9401.
[3] Su XL, Wang M, Yan ZH, et al. Quantum network based on non-classical light. Sci China Inf Sci. 2020;63:1–12.
[4] Hosseini M, Sparkes BM, Campbell G, et al. High efficiency coherent optical memory with warm rubidium vapour. Nat commun. 2011;2:1–5.
[5] Parigi V, Ambrosio V, Arnold C, et al. Storage and retrieval of vector beams of light in a multiple-degree-of-freedom quantum memory. Nat Commun. 2015;6:7706.
[6] Yan ZH, Jia XJ. Quantum manipulation and enhancement of deterministic entanglement between atomic ensemble and light via coherent feedback control. *Quantum Sci. Technol.* 2017; 2:024003.
[7] Pu YF, Jiang N, Chang W, et al. Experimental realization of a multiplexed quantum memory with 225 individually accessible memory cells. Nat Commun. 2017;8:15359.
[8] Colangelo G, Ciurana FM, Bianchet LC, et al. Simultaneous tracking of spin angle and amplitude beyond classical limits. Nature. 2017;543:525–528.

[9] Specht HP, Nölleke C, Reiserer A, et al. A single-atom quantum memory. Nature. 2011;473:190–193.
[10] Facon A, Dietsche EK, Grosso D, et al. A sensitive electrometer based on a Rydberg atom in a Schrödinger-cat state. Nature. 2016;535:262–265.
[11] Stute A, Casabone B, Schindler P, et al. Tunable ion–photon entanglement in an optical cavity. Nature. 2012;485:482–485.
[12] Hucul D, Inlek IV, Vittorini G, et al. Modular entanglement of atomic qubits using photons and phonons. Nat Phys. 2015;11:37–42.
[13] Flurin E, Roch N, Pillet JD, et al. Superconducting quantum node for entanglement and storage of microwave radiation. Phys Rev Lett. 2015;114:090503.
[14] Fiore V, Yang Y, Kuzyk MC, et al. Storing optical information as a mechanical excitation in a silica optomechanical resonator. Phys Rev Lett. 2011;107:133601.
[15] Lee H, Suh MG, Chen T, et al. Spiral resonators for on-chip laser frequency stabilization. Nat commun. 2013;4:1–6.
[16] Riedinger R, Hong S, Norte RA, et al. Non-classical correlations between single photons and phonons from a mechanical oscillator. Nature. 2016;530:313–316.
[17] Kiesewetter S, Teh RY, Drummond PD, et al. Pulsed entanglement of two optomechanical oscillators and furry's hypothesis. Phys Rev Lett. 2017;119:023601.
[18] Saglamyurek E, Sinclair N, Jin J, et al. Broadband waveguide quantum memory for entangled photons. Nature. 2011;469:512–515.
[19] Zhong M, Hedges MP, Ahlefeldt RL, et al. Optically addressable nuclear spins in a solid with a six-hour coherence time. Nature. 2015;517:177–180.
[20] Duan LM, Lukin MD, Cirac JI, et al. Long-distance quantum communication with atomic ensembles and linear optics. Nature. 2001;414:413–418.
[21] Daiss S, Langenfeld S, Welte S, et al. A quantum-logic gate between distant quantum-network modules. Science. 2021;371:614–617.
[22] Bao H, Duan J, Jin S, et al. Spin squeezing of 1011 atoms by prediction and retrodiction measurements. Nature. 2020;581:159–163.
[23] Fleischhauer M, Imamoglu A, Marangos JP. Electromagnetically induced transparency: optics in coherent media. Rev Mod Phys. 2005;77:633.
[24] Phillips DF, Fleischhauer A, Mair A, et al. Storage of light in atomic vapor. Phys Rev Lett. 2001;86:783.
[25] Fleischhauer M, Lukin MD. Quantum memory for photons: dark-state polaritons. Phys Rev A. 2002;65:022314.
[26] Julsgaard B, Sherson J, Cirac JI, et al. Experimental demonstration of quantum memory for light. Nature. 2004;432:482–486.
[27] Hétet G, Longdell JJ, Sellars MJ, et al. Multimodal properties and dynamics of gradient echo quantum memory. Phys Rev Lett. 2008;101:203601.
[28] Moiseev SA, Kröll S. Complete reconstruction of the quantum state of a single-photon wave packet absorbed by a doppler-broadened transition. Phys Rev Lett. 2001;87:173601.
[29] Afzelius M, Gisin N, De-riedmatten H, et al. A solid-state light–matter interface at the single-photon level. Nature. 2008;456:773–777.
[30] Yuan ZS, Chen YA, Zhao B, et al. Experimental demonstration of a BDCZ quantum repeater node. Nature. 2008;454:1098–1101.
[31] Heller L, Farrera P, Heinze G, et al. Cold-atom temporally multiplexed quantum memory with cavity-enhanced noise suppression. Phys Rev Lett. 2020;124:210504.
[32] Fleischhauer M, Lukin MD. Dark-state polaritons in electromagnetically induced transparency. Phys Rev Lett. 2000;84:5094.

[33] Cviklinski J, Ortalo J, Laurat J, et al. Reversible quantum interface for tunable single-sideband modulation. Phys Rev Lett. 2008;101:133601.
[34] Katz O, Firstenberg O. Light storage for one second in room-temperature alkali vapor. Nat commun. 2018;9:1–6.
[35] Novikova I, Gorshkov AV, Phillips DF, et al. Optimal control of light pulse storage and retrieval. Phys Rev Lett. 2007;98:243602.
[36] Hsiao YF, Tsai PJ, Chen HS, et al. Highly efficient coherent optical memory based on electromagnetically induced transparency. Phys Rev Lett. 2018;120:183602.
[37] Vernaz-Gris P, Huang K, Cao M, et al. Highly-efficient quantum memory for polarization qubits in a spatially-multiplexed cold atomic ensemble. Nat commun. 2018;9:1–6.
[38] Schraft D, Hain M, Lorenz N, et al. Stopped Light at High Storage Efficiency in a Pr 3 + Y 2 SiO 5 Crystal. Phys Rev Lett. 2016;116:073602.
[39] Wang YF, Li JF, Zhang SC, et al. Efficient quantum memory for single-photon polarization qubits. Nat Photon. 2019;13:346.
[40] Pan JW, Chen ZB, Lu CY, et al. Multiphoton entanglement and interferometry. Rev Mod Phys. 2012;84:777.
[41] Braunstein SL, Van-Loock P. Quantum information with continuous variables. Rev Mod Phys. 2005;77:513.
[42] Yan Z-H, Qin J-L, Qin -Z-Z, et al. Generation of non-classical states of light and their application in deterministic quantum teleportation. *Fundamental Res*. 2021; 1: 43–49.
[43] Wu LA, Kimble HJ, Hall JL, et al. Generation of squeezed states by parametric down conversion. Phys Rev Lett. 1986;57:2520.
[44] Ou ZY, Pereira SF, Kimble HJ, et al. Realization of the Einstein-Podolsky-Rosen paradox for continuous variables. Phys Rev Lett. 1992;68:3663.
[45] Cai XD, Wu D, Su ZE, et al. Entanglement-based machine learning on a quantum computer. Phys Rev Lett. 2015;114:110504.
[46] Su XL, Hao SH, Deng XW, et al. Gate sequence for continuous variable one-way quantum computation. Nat Commun. 2013;4:1–9.
[47] Chen YA, Zhang AN, Zhao Z, et al. Experimental quantum secret sharing and third-man quantum cryptography. Phys Rev Lett. 2005;95:200502.
[48] Lance AM, Symul T, Bowen WP, et al. Tripartite quantum state sharing. Phys Rev Lett. 2004;92:177903.
[49] Zhou YY, Yu J, Yan ZH, et al. Quantum secret sharing among four players using multipartite bound entanglement of an optical field. Phys Rev Lett. 2018;121:150502.
[50] Bouwmeester D, Pan JW, Mattle K, et al. Experimental quantum teleportation. Nature. 1997;390:575–579.
[51] Furusawa A, Sørensen JL, Braunstein SL, et al. Unconditional quantum teleportation. Science. 1998;282:706–709.
[52] Pan JW, Bouwmeester D, Weinfurter H, et al. Experimental entanglement swapping: entangling photons that never interacted. Phys Rev Lett. 1998;80:3891.
[53] Jia XJ, Su XL, Pan Q, et al. Experimental demonstration of unconditional entanglement swapping for continuous variables. Phys Rev Lett. 2004;93:250503.
[54] Zuo XJ, Yan ZH, Feng YN, et al. Quantum interferometer combining squeezing and parametric amplification. Phys Rev Lett. 2020;124:173602.
[55] Iskhakov TS, Agafonov IN, Chekhova MV, et al. Polarization-Entangled light pulses of 10 $^{5}$ photons. Phys Rev Lett. 2012;109:150502.
[56] Jensen K, Wasilewski W, Krauter H, et al. Quantum memory for entangled continuous-variable states. Nat Phys. 2011;7:13–16.

[57] Appel J, Figueroa E, Korystov D, et al. Quantum memory for squeezed light. Phys Rev Lett. 2008;100:093602.
[58] Honda K, Akamatsu D, Arikawa M, et al. Storage and retrieval of a squeezed vacuum. Phys Rev Lett. 2008;100:093601.
[59] Choi KS, Deng H, Laurat J, et al. Mapping photonic entanglement into and out of a quantum memory. Nature. 2008;452:67–71.
[60] Ladd TD, Jelezko F, Laflamme R, et al. Quantum computers. Nature. 2010;464:45–53.
[61] Sangouard N, Simon C, De Riedmatten H, et al. Quantum repeaters based on atomic ensembles and linear optics. Rev Mod Phys. 2011;83:33.
[62] Kimble HJ. The quantum internet. Nature. 2008;453:1023–1030.
[63] Yan ZH, Wu L, Jia XJ, et al. Establishing and storing of deterministic quantum entanglement among three distant atomic ensembles. Nat Commun. 2017;8:1–8.
[64] Yan ZH, Wu L, Jia XJ, et al. Quantum entanglement among multiple memories for continuous variables. Adv Quantum Technol. 2021;4:2100071.
[65] Lukin MD. Colloquium:trapping and manipulating photon states in atomic ensembles. Rev Mod Phys. 2003;75:457.
[66] Boller KJ, Imamoğlu A, Harris SE. Observation of electromagnetically induced transparency. Phys Rev Lett. 1991;66:2593.
[67] Moseley RR, Sinclair BD, Dunn MH. Local field effect in the three-level atom. Opt Commun. 1994;108:247–252.
[68] Harris SE, Field JE, Kasapi A. Dispersive properties of electromagnetically induced transparency. Phys Rev A. 1992;46:R29.
[69] Kasapi A, Jain M, Yin GY, et al. Electromagnetically induced transparency:propagation dynamics. Phys Rev Lett. 1995;74:2447.
[70] Hau L, Harris S, Dutton Z, et al. Light speed reduction to 17 metres per second in an ultracold atomic gas. Nature. 1999;397:594–598.
[71] Kash MM, Sautenkov VA, Zibrov AS, et al. Ultraslow group velocity and enhanced nonlinear optical effects in a coherently driven hot atomic gas. Phys Rev Lett. 1999;82:5229.
[72] Budker D, Kimball DF, Rochester SM, et al. Nonlinear magneto-optics and reduced group velocity of light in atomic vapor with slow ground state relaxation. Phys Rev Lett. 1999;83:1767.
[73] Gorshkov AV, André A, Fleischhauer M, et al. Universal approach to optimal photon storage in atomic media. Phys Rev Lett. 2007;98:123601.
[74] Zhang Q, Huang G. Suppression of quantum noise by two-mode squeezed states for photon propagation under conditions of electromagnetically induced transparency and four-wave mixing. Phys Rev A. 2020;101:033806.
[75] Zhang R, Wang X-B. Storage efficiency of probe pulses in an electromagnetically-induced-transparency medium. Phys Rev A. 2016;94:063856.
[76] Zhang Q, Huang G. Quantum memory of single-photon polarization qubits via double electromagnetically induced transparency. Phys Rev A. 2021;104:033714.
[77] Maxwell D, Szwer DJ, Paredes-Barato D, et al. Storage and control of optical photons using rydberg polaritons. Phys Rev Lett. 2013;110:103001.
[78] Li L, Kuzmich A. Quantum memory with strong and controllable Rydberg-level interactions. Nature Communications. 2016;7:1–5.
[79] Tian XD, Liu YM, Bao QQ, et al. Nonclassical storage and retrieval of a multiphoton pulse in cold rydberg atoms. Phys Rev A. 2018;97:043811.
[80] Bai Z, Li W, Huang G. Stable single light bullets and vortices and their active control in cold Rydberg gases. Optica. 2019;6:309–317.

[81] Shou C, Zhang Q, Luo W, et al. Photon storage and routing in quantum dots with spin-orbit coupling. Opt Express. 2021;29:9772–9785.
[82] Chen Y, Bai Z, Huang G. Ultraslow optical solitons and their storage and retrieval in an ultracold ladder-type atomic system. Phys Rev A. 2014;89:023835.
[83] Chen Y, Chen Z, Huang G. Storage and retrieval of vector optical solitons via double electromagnetically induced transparency. Phys Rev A. 2015;91:023820.
[84] Shou C, Huang G. Storage and retrieval of slow-light dark solitons. Opt Lett. 2020;45:6787–6790.
[85] Su J, Xu D, Huang G. Storage and retrieval of surface polaritons. ACS Photonics. 2018;5:2496–2502.
[86] Phillips NB, Gorshkov AV, Novikova I. Optimal light storage in atomic vapor. Phys Rev A. 2008;78:023801.
[87] Novikova I, Phillips NB, Gorshkov AV. Optimal light storage with full pulse-shape control. Phys Rev A. 2008;78:021802.
[88] Chen YH, Lee MJ, Wang IC, et al. Coherent optical memory with high storage efficiency and large fractional delay. Phys Rev Lett. 2013;110:083601.
[89] Xu ZX, Wu YL, Tian L, et al. Long lifetime and high-fidelity quantum memory of photonic polarization qubit by lifting zeeman degeneracy. Phys Rev Lett. 2013;111:240503.
[90] Lauk N, O'Brien C, Fleischhauer M. Fidelity of photon propagation in electromagnetically induced transparency in the presence of four-wave mixing. Phys Rev A. 2013;88:013823.
[91] Hedges MP, Longdell JJ, Li YM, et al. Efficient quantum memory for light. Nature. 2010;465:1052–1056.
[92] Zhou ZQ, Lin WB, Yang M, et al. Realization of reliable solid-state quantum memory for photonic polarization qubit. Phys Rev Lett. 2012;108:190505.
[93] Saglamyurek E, Puigibert MG, Zhou Q, et al. A multiplexed light-matter interface for fibre-based quantum networks. Nat commun. 2016;7:1–7.
[94] Heinze G, Hubrich C, Halfmann T. Stopped light and image storage by electromagnetically induced transparency up to the regime of one minute. Phys Rev Lett. 2013;111:033601.
[95] Knill E, Laflamme RM, J G. A scheme for efficient quantum computation with linear optics. Nature. 2001;409:46–52.
[96] Zhang S, Chen JF, Liu C, et al. A dark-line two-dimensional magneto-optical trap of 85 Rb atoms with high optical depth. Rev Sci Instrum. 2012;83:073102.
[97] Geng J, Campbell GT, Bernu J, et al. Electromagnetically induced transparency and four-wave mixing in a cold atomic ensemble with large optical depth. New J Phys. 2014;16:113053.
[98] Kolchin P, Belthangady C, Du S, et al. Electro-optic modulation of single photons. Phys Rev Lett. 2008;101:103601.
[99] Chen JF, Zhang S, Yan H, et al. Shaping biphoton temporal waveforms with modulated classical fields. Phys Rev Lett. 2010;104:183604.
[100] Appel J, Hoffman D, Figueroa E, et al. Electronic noise in optical homodyne tomography. Phys Rev A. 2007;75:035802.
[101] Arikawa M, Honda K, Akamatsu D, et al. Observation of electromagnetically induced transparency for a squeezed vacuum with the time domain method. Opt Express. 2007;15:11849–11854.
[102] Hansen H, Aichele T, Hettich C, et al. Ultrasensitive pulsed, balanced homodyne detector: application to time-domain quantum measurements. Opt Lett. 2001;26:1714–1716.

[103] Neergaard-Nielsen JS, Nielsen BM, Hettich C, et al. Generation of a superposition of odd photon number states for quantum information networks. Phys Rev Lett. 2006;97:083604.
[104] Takei N, Lee N, Moriyama D, et al. Time-gated Einstein-Podolsky-Rosen correlation. Phys Rev A. 2006;74:060101.
[105] Tan SM, Walls DF, Collett MJ. Nonlocality of a single photon. Phys Rev Lett. 1991;66:252–255.
[106] Hessmo B, Usachev P, Hoshang H, et al. Experimental demonstration of single photon nonlocality. Phys Rev Lett. 2004;92:180401.
[107] Jacques V, Wu E, Grosshans F, et al. Experimental realization of wheeler's delayed-choice gedanken experiment. Science. 2007;315:966–968.
[108] Laurat J, Chou CW, Deng H, et al. Towards experimental entanglement connection with atomic ensembles in the single excitation regime. New J Phys. 2007;9:207–220.
[109] Van Loock P, Furusawa A. Detecting genuine multipartite continuous variable entanglement. Phys Rev A. 2003;67:052315.
[110] Wu L, Yan ZH, Liu YH, et al. Experimental generation of tripartite polarization entangled states of bright optical beams. Appl Phys Lett. 2016;108:161102.
[111] Ou ZY. Efficient conversion between photons and between photon and atom by stimulated emission. Phys Rev A. 2008;78:023819.
[112] He QY, Reid MD, Giacobino E, et al. Dynamical oscillator-cavity model for quantum memories. Phys Rev A. 2009;79:022310.
[113] Yang SJ, Wang XJ, Bao XH, et al. An efficient quantum light–matter interface with sub-second lifetime. Nat Photon. 2016;10:381–384.
[114] Saunders DJ, Munns JHD, Champion TFM, et al. Cavity-enhanced room-temperature broadband raman memory. Phys Rev Lett. 2016;116:090501.
[115] Awschalom D, Berggren KK, Bernien H, et al. Development of quantum interconnects (quics) for next-generation information technologies. *PRX Quantum*. 2021; 2: 017002.
[116] Hedges MP, Longdell JJ, Li Y, et al. Efficient quantum memory for light. Nature. 2010;465:1052–1056.